Open Access Article

The Influence of Urbanism on the Urban Heat Island Phenomenon: Evidence from the KSA

Ammar Maghrabi[1,2*], Mohd Farid Mohamed[1], Sudharshan N. Raman[3], Mohd Khairul Azhar Mat Sulaiman[1], Wardah Fatimah Mohammad Yusoff[1], Mohammed Awad Abuhussain[4], Mansour Almazroui[5]

[1] Department of Architecture and Built Environment, Universiti Kebangsaan Malaysia, Bangi, Malaysia

[2] Institute for Hajj and Umrah Research, Umm Al Qura University, Mecca, Saudi Arabia

[3] Civil Engineering Discipline, School of Engineering, Monash University Malaysia, Selangor, Malaysia

[4] Department of Architectural Engineering, Najran University, Najran, Saudi Arabia

[5] Department of Meteorology, King Abdulaziz University, Jeddah, Saudi Arabia

Abstract: The density and pattern of urban development can significantly influence the thermal environment in these areas. Several research studies have underlined the asymmetry of urban air temperature by using parameters such as an increase in mean temperature, decline in amplitude, and substantial phase delay in closely constructed buildings. This research examines urban morphological impacts on the city thermal climate using the data collected on air temperature. The data for this study were collected using iButton data loggers implemented across two different locations representing urban and suburban areas. Also, the study utilized one meteorological station to archive the climatic information in a rural area as a reference point. The data collection camping was held in 2019 during June, July, and August, which are considered the hottest months of the year at the case study location. The iButton data loggers were validated by calibrating the readings in a room chamber at the University Kbangsaan Malaysia (UKM) Malaysia. The study includes data analysis for the micro weather profile for all locations, including daytime, nighttime, and daily average air temperature. Results from the study indicated that daytime and nighttime temperature variation among urban and rural areas reached 3.6℃ and 6.3℃, respectively.

Keywords: urban heat island, Makkah, Saudi Arabia, temperature.

城市化對城市熱島現象的影響：來自沙特阿拉伯王国的證據

摘要：城市發展的密度和模式可以顯著影響這些地區的熱環境。使用諸如平均溫度升高、振幅下降和緊密建造的建築物的顯著相位延遲等參數，一些研究強調了城市氣溫的不對稱性。本研究旨在利用收集到的氣溫數據來檢驗城市形態對城市熱氣候的影響。本研究的數據是使用按钮數據記錄器收集的，這些記錄器在代表城市和郊區的兩個不同位置實施。此外，該研究利用一個氣象站將農村地區的氣候信息存檔為參考點。數據收集露營於 2019 年在 6 月、7 月和 8 月舉行，這些月份被認為是案例研究地點一年中最熱的月份。按钮數據記錄器通過在馬來西亞邦桑大學 (联合王国) 馬來西亞校準房間內的讀數進行驗證。該研究包括對所有地點的微觀天氣概況的數據分析，包括白天、夜間和每日平均氣溫。研究結果表明，城鄉晝夜溫差分別達到 3.6℃和 6.3℃.

Received: June 4, 2021 / Revised: August 7, 2021 / Accepted: September 5, 2021 / Published: October 30, 2021

About the authors: Ammar Maghrabi, Department of Architecture and Built Environment, Universiti Kebangsaan Malaysia, Bangi, Malaysia; Institute for Hajj and Umrah Research, Umm Al Qura University, Mecca, Saudi Arabia; Mohd Farid Mohamed, Department of Architecture and Built Environment, Universiti Kebangsaan Malaysia, Bangi, Malaysia; Sudharshan N. Raman, Civil Engineering Discipline, School of Engineering, Monash University Malaysia, Selangor, Malaysia; Mohd Khairul Azhar Mat Sulaiman, Wardah Fatimah Mohammad Yusoff, Department of Architecture and Built Environment, Universiti Kebangsaan Malaysia, Bangi, Malaysia; Mohammed Awad Abuhussain, Department of Architectural Engineering, Najran University, Najran, Saudi Arabia; Mansour Almazroui, Department of Meteorology, King Abdulaziz University, Jeddah, Saudi Arabia

Corresponding author Ammar Maghrabi, ammar_maghrabi@hotmail.com

关键词：城市熱島, 麥加, 沙特阿拉伯, 溫度.

1. Introduction

In 2007, research studies showed that the population of urban dwellers across the globe was over 50%, and this was projected to reach up to 70% by 2050 [1]. A high rate of urbanization and industrial growth is expected to follow economic and human population growth, consequent upon the need for comfort and a good standard of living. Population increase in a metropolitan is usually accompanied by removal of ground vegetation and land cover to accommodate further expansion in the area. The conversion of natural ground cover to artificial surfaces will lead to higher heat retention during the summer and on days with intense sunshine. Rapid urbanization leads to considerable changes in the climates of urban areas. This phenomenon is known as urban heat island (UHI), in which the air temperature in typical urban areas is higher compared to their adjacent rural environment [2]. According to [3], the urban heat island is the difference in air temperature between a metropolitan and a rural area. It is expected that temperature increase must follow a gradual progression from the outskirt of the city to the center of the urban area where the highest temperature is expected [4, 5]. This difference in air temperature between the city and its adjacent rural area is described as Urban Heat Island Intensity (UHII), used to predict urban heat island intensity in an environment [6]. As the name describes, the phenomenon of urban heat island is commonly applied to cities as these metropolitan areas commonly have surfaces with features such as high heat storage capacity, high impermeability, low albedo, and low sky view factor [7]. Research studies have identified several factors responsible for the urban heat island, and these factors have been grouped into four main categories [6]. The categories include geographical location and climate of an environment; regional- and city-scale features, such as vegetation, land use, topography, morphology, and demography; local characteristics that affect the temperature, including the structure, surfaces, and buildings characteristics, as well as anthropogenic activities [8], and meteorological factors such as solar radiation, rainfall cloud cover, and wind.

Over the past few decades, the phenomena of UHI have been extensively studied. The variation of air temperature, precipitation, surface energy flux, wind speed and direction, humidity, etc., are some parameters that experts have analyzed to document the extent of the UHI [9, 10]. In the 1970s, a major US campaign was held, and so-called The Metropolitan Meteorological Experiment (METROMEX). The researcher used advanced equipment such as rain radars and aircraft flights to study the hydrological cycle of a specific environment while considering the impact of rain formation resulting from urban induced moisture convergence [11]. Lately, several research studies have been conducted on the UHI effects across different cities of the world, such as in Manchester, UK [12] Modena, Italy [13] Shanghai, China [14] Toronto, Canada [15] and Riyadh, Saudi Arabia [16]. Assessment of long-term temperature data has shown that the effect of urban growth on air temperature is not only restricted to densely populated urban environments; it has been recorded in cities with a lesser human population [17]. Due to the UHI phenomenon, industrial and metropolitans' central areas are characterized by higher micro-climate that negatively contribute to the thermal environment by increasing the air temperature [18, 19].

Extensive studies have been conducted on the UHI phenomenon using different measuring techniques. The techniques for measuring UHI have been grouped into three major categories viz; remote sensing technique [20], modeling technique [2, 5, 18], and on-site measurements [21]. Challenges may arise in UHI measurement due to the shortage of air temperature data with clear spatial resolutions and extensive spatial coverages. Information on air temperature over a large expanse is obtained through remote sensing from the satellite. However, the data obtained may be of lower resolution than required [22]. High-resolution imaging is very important in UHI studies since the research on the UHI phenomenon requires a comparison of the microclimate of two or more areas. The in-situ method of UHI measurement entails the on-site collection of weather information from a vantage point or automatic weather stations situated at different areas of the locations under study. The selected areas must represent the urban and rural areas of a city [23]. The onsite modeling method offers the advantage of the ease in control, testing, and validation, and it could it has types of campaigns. The first campaign, described as the fixed campaign, entails collecting meteorological data from different stations in the study location. Meanwhile, the second campaign, called the mobile campaign, describes the method of weather data collection in an area while on foot or in a vehicle [18].

Theoretically, UHII can be characterized by measuring surface temperature or air temperature [23, 13, 24]. This phenomenon has been approved to be influenced not only by daytime but also nighttime hours. Even though the temperature may have similar readings during daytime when comparing rural and urban areas, the nighttime-hours microclimate profile has a higher air and surface temperature [25]. The air or surface temperature variation could be attributed to heat gain,

anthropogenic heat, and solar radiation stored in the surrounding thermal mass [25, 26].

Globally, the significance of the UHI consequences is strongly witnessed on building performance. In Rome and Beijing, UHI has been estimated to rias cooling energy consumption by 30% and 11%, respectively [27, 28]. Previous studies have estimated the increase of electricity demand to be between 0.45% and 4.6% per degree of UHII, in addition to overall energy consumption increase range between 0.5% and 8.5% per degree [29]. In the Kingdom of Saudi Arabia (KSA), where the case study is located, the electricity generation has reached 60 GW in the summer of 2015 compared to 23 GW in the winter season [30]. Each 1°C increase in air temperature is argued to be responsible for additional electricity generation of 1.18 GW [31]. In KSA, during 2018, nearly half of the total electricity generated was consumed by the residential sector, and more than 65% of it was consumed for the cooling demands [31, 34]. The rapid growth in the national economy has led to a consequent increase in urbanization in most cities of KSA due to the increased availability of funds for infrastructural development across all sectors of the country [33, 34]. Over the last thirty years, considerable growth, innovations, and complexity have been witnessed in city structure due to the growing human population, government policies, and unsystematic development. The perennial increase in the population of city inhabitants can be attributed to the movement of people to the city in the quest for better living and work opportunities.

Alqurashi et al., (35) analyzed the urban growth of five cities in Saudi Arabia. It was observed that the highest transition probability in the western region, including Makkah city, is the change from vegetation cover to urban construction. The study also shows that Makkah is one of the most urbanized and populated cities in the country.

Due to urban migration to the western region where Makkah city is located, the total electricity consumption from 2009-2018 increased from 65.292 GWh to 101.159 GWh, which is considered the highest energy consumption increase among regions in the country [36]. The present research consists of a three-month data collection exercise to collect meteorological data in Makkah, KSA. The campaign was conducted across three locations in the city, each representing the urban, suburban, and rural areas from which hourly temperature data was collected. The main aim of the current study is to investigate the variation of ambient air temperature (Ta) among urban, suburban, and rural areas within the context of Makkah city.

2. Literature Review

Makkah is considered the Islamic capital of KSA and worship center for Muslims worldwide. It witnesses the influx of Muslims who come to perform Umrah and Hajj in compliance with the dictate of Islam. Data from the Umrah Survey for “Internal worshipper” as well as information obtained from the Ministry of Hajj and Umrah for the “Abroad worshipper” shows that in 2019 over 2.300.000 pilgrims visited the city of Makkah to perform their Islamic rite [37]. By 2030, the pilgrims' number is visioned to reach approximately 4 million annually [38]. The focal point of the central area of Makkah is the Holy Mosque which is located in the lower point in med of mountain areas with a square shape. Surrounding the Holy Mosque is a huge accommodation area filled with hotels, malls, service centers, and residential area. With compliance to the increase of visitor number to the city of Makkah, the central area with the Holy Mosque has been under rapid process of expansion in the last 30 years. The expansion included expanding the Holy Mosque to accommodate more worshipers, and as a consequence expanding the development in the surrounding areas [38]. Figure 1 shows the central area for 30 years.

The city of Makkah lies in the southwestern part of KSA, about 70 km east of the Red Sea. The land area of Makkah city extends from 39° 35' E to 40° 02' E longitudes and 21° 09' N to 21° 37' N latitudes, with the city having several geological elevations existing within its boundaries [39]. The city's elevation ranges from 82 to 982 meters above sea level, with developmental activities concentrated mostly in the low land due to the economic potentials of the area [40].

KSA climate can be described as a hot and dry desert following the Koppen-Geiger system of classification. This is represented by the symbol BWh, where “B” shows that the land is arid, “W” indicates that rainfall in the area is usually during the winter, while “h” signifies that the climate of the location is hot and dry except in the southwestern highlands [41, 42].

The climate of Makkah is characterized as hot and dry with low humidity (12 days of rainfall in a year). The hottest months in the city usually extend from May to October, where the temperature in July may rise to over 45 ℃ [43]. The coolest months are usually between November and April, where the mean monthly temperature ranges between 23 ℃ to 27℃ [44]. The average highest, lowest, and mean monthly dry-bulb temperature for Makkah is presented in Fig. 1 and 2.

Fig. 1 A. Visual image of the central areas of Makkah in 2005; B. Visual image of the central areas of Makkah in 2020

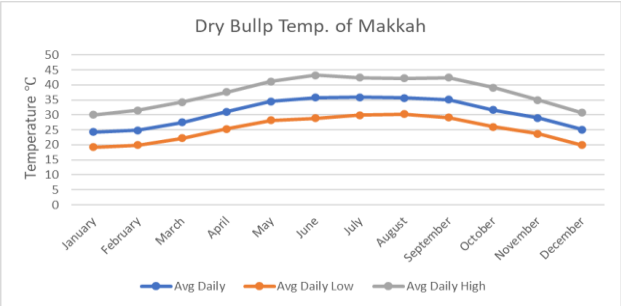

Fig. 2 Average dry bullp temp. of Makkah

2.1. Energy Trend and Building Sector in the Context of Saudi Arabia

In recent times, there has been a remarkable increase in energy consumption per capita of the world's population, particularly in advanced nations of the world. One of the reasons for the increase is the high rate of urbanization which impacts the country's environmental profile. The effect of this urbanization is that it can foster or destroy the general concept of a nation's green environment. According to [45], the economic development of a country is usually accompanied by the large influence of industrialization, which leaves an imprint on the environment. Data collected from several countries between 1970–2000 showed that 1% increase in industrialization activities could result in about 11% emissions per capita. This was consistent with [46], who reported in their study that industrialization can have a short and long-term impact on the environment. The researchers further established that there is a causal relationship between urbanization, industrialization, and CO2 emissions. The results show that it is necessary to manage industrialization activities to balance industry-related activities and environmental structure. This would help to improve energy efficiency and technological innovation [47].

There are plenty of non-renewable and renewable energy sources in Saudi Arabia. The British Petroleum Statistical Review of World Energy reported that Saudi Arabia is the world's 2nd and 6th largest holder of proved oil reserves and natural gas reserves, respectively, having about 36.5 thousand million tons, i.e., 15.9% of the global oil reserve [48]. Nevertheless, Saudi Arabia was ranked top in global oil production, with 547.0 million tons of oil produced in 2012 accounting for 13.3% of the global oil production. Meanwhile, the country is ranked 20th in terms of global electricity consumption and 6th in terms of global consumption of oil and natural gas [48]. In other terms, Saudi Arabia is ranked top amongst countries with energy consumption levels above the global average with 129.7 and 92.5 million tons of oil and natural gas used in 2012.

The remarkable production rate and consumption level of petroleum products and natural gases in the country are accompanied by CO_2 emissions. The country ranked the ninth-largest in terms of CO2 emissions (2.8% of total world emissions) [49]. Despite the economic diversification efforts embarked upon by Saudi Arabia, the oil industry remains the mainstream of its economy, accounting for about 45% of GDP, 75% of budget revenues, and 90% of exports earnings [50]. The growth rates of real GDP per capita, energy consumption per capita, and CO2 emissions per capita from 1971–2010 are presented in .

Table 1 Growth rates of real GDP per capita, energy consumption per capita, and CO2 emission per capita in KSA

Variables	1971-1980	1981-1990	1991-2000	2001-2010	1971-2010
Growth rate of real GDP per capita	79.01	-42.06	-0.41	28.51	33.59
Growth rate of Energy consumption per capita	159.97	-8.62	21.07	19.60	406.3
Growth rate of CO2 consumption per capita	74.22	-19.65	-7.78	13.44	64.32

Saudi Arabia witnessed massive economic prosperity from the late 1970s to 1980, with a nearly 80% real GDP per capita increase. However, in 2001–2010, real GDP per capita only increased by 28.51%. Meanwhile, energy consumption per capita in Saudi Arabia was three-fold times higher than the world average at 6.168 tons in 2010, while the country has recorded a 405.3% increase in energy consumption per capita from 1971-2010. Also, CO_2 emissions per capita from 1971–1980 were higher than the rate recorded from 2001–2010. Despite Saudi's agreement in the Kyoto Protocol of 2005 to manage and reduce CO_2 emissions, a nearly 14% increase in CO2 emissions per capita was recorded between 2001 and 2010. During the period under discussion, it was observed that energy consumption per capita increased faster compared to the other variables, and the highest difference was observed between the growth of energy consumption per capita and real GDP per capita [49]. One of the main sectors that witnessed a great increase in energy consumption in Saudi Arabia is the building sector, which will be separately discussed in the next section

2.1.1. Observational Approaches of UHI Phenomenon

The most common method of examining the UHI phenomenon is through sensors to measure ambient air temperature in a particular place over a given time frame. The UHI intensity is evaluated by comparing the ambient temperature measured in an urban settlement against air temperature in an adjacent rural area [51]. The UHI phenomenon has been the focus of numerous studies conducted over the past years. Several parameters have been considered and studied by experts in their attempt to evaluate the severity of UHI. These include rainfall, differences in air temperature, humidity, surface energy flux, wind speed, and direction [9, 52, 53, 54, 55, 56, 10]. During the 1970s, The Metropolitan Meteorological Experiment

(METROMEX) was launched as a major campaign on UHI in the United States. The researcher used state-of-the-art equipment such as rain radars and aircraft flights to evaluate the hydrological cycle of environments while considering the impact of rain formation that resulted from urban induced moisture convergence [57]. The first field measurement of UHI was conducted in London by Howard in 1818 [58]. Similarly, the UHI scenario in Athens was evaluated from twenty-three experimental sites in Athens' urban and suburban regions to record the ambient air temperature and humidity from 1997 to 1998 [11, 57]. In recent times, extensive research studies have been carried out to study UHI effects in different regions of the world such as, in Manchester, UK [12], Modena, Italy [13], Shanghai, China [14], Toronto, Canada [15] and Riyadh, Saudi Arabia [59]. A recent study on UHI in London, UK, used different measuring points within the London metropolis. The researcher compared the values recorded in these areas to the reference location, i.e., the London Heathrow Airport [60] (See Figure 3-5). These different measurement locations were chosen considering their proximity to the Central metropolis.

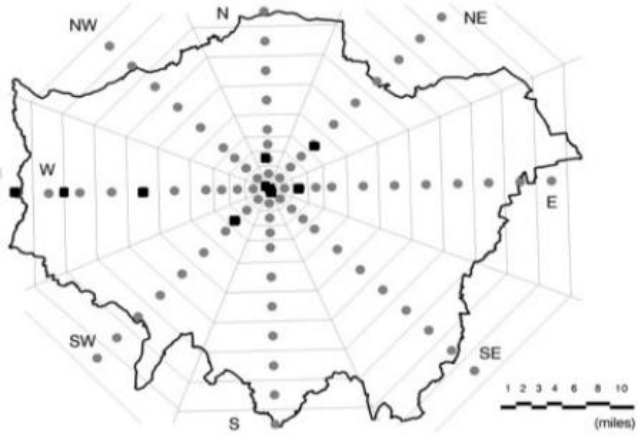

Fig. 3 On-site temperature stations on Grater London [58]

Another approach to the study of UHI is through the use of automobiles. Sundborg, in 1950 researched the local climate of Uppsala, Sweden, using a thermometer mounted on a vehicle to give a spatial picture of the urban heat island [61]. **Ошибка! Источник ссылки не найден.** shows the instrument mounted on the top of a car.

3. Research Methodology

The UHI phenomenon in Makkah was studied using i-Button Data Logger (DS1923-F5) and one metrological station, Hada Al-sham station. Three different locations were selected that represent the urban, suburban, and rural areas. The study used the ambient air temperature and relative humidity data as major parameters to understand the microclimate variation among all selected locations. At the urban and suburban locations, i-Button Data Logger (DS1923-F5) was situated free-standing 10-14 meters above ground level on the top of residential buildings. In contrast, in the rural area, meteorological data from the Hada Alsham weather station were utilized. Temperature and humidity sensors of the Hada Alsham weather station are situated at 10 meters above ground level. Distance from the urban location is 16.3 KM and 46 KM for the suburban and rural areas, respectively. The data for the study were collected between June -August 2019, which represents the hottest months of the year.

3.1. Site Selection

The distinguished research areas in the city of Makkah into urban, suburban, and rural areas Figure 3, thereby controlling geographical differences between places in the city. The major criteria used in classifying the area is their distance from the center of the city. This has been identified as one of the major factors affecting UHI formation [60]. Several site visits to assess the level of development, urban growth patterns, and buffer zones confirm the accuracy of the researcher's classification of Makkah city. Thus, the three different sites were selected to represent the urban, suburban, and rural areas to study the temperature variation in the city.

The effect of density on the thermal environment in the built-up area was evaluated in the urban and suburban configurations. The urban area is characterized by multiple use district consisting of residential and commercial buildings, whereas the suburban configuration represents an urban area set aside only for residential purposes. The layout for the urban area consists of narrow streets with storied buildings of various sizes. In contrast, the suburban configuration consists of broad streets with detached two to four-storied buildings with setbacks from streets (around one-fifth of the street’s width). The rural configuration for this study is situated in the northern part of Makkah, about 46km from the urban area.

3.2. Equipment and Validation

The data utilized in this study were collected using the i-Button Data Logger (DS1923-F5) in urban and suburban. In contrast, data on the rural area were collected from the Hada Al-sham metrological station. The selection of the i-Button Data Logger (DS1923-F5) was made after ensuring that the loggers are appropriate in terms of storage capacity, life span, and archiving data. One i-Button Data Logger (DS1923-F5) was installed at the top of a residential building (Figure 4) for each urban and suburban areas as the device was found to satisfy the criteria of the data logger specification (Table 1). Both data loggers were set up to collect hourly measurements of ambient air temperature and relative humidity from the 01st of June to the 31st of August. In the rural area, there were limitations in implementing the i-Button Data Logger DS1923-F5. Thus, hourly data on temperature and relative humidity for the period under consideration were collected from Hada Al-sham metrological station. Table 2 includes details measuring related information for all locations.

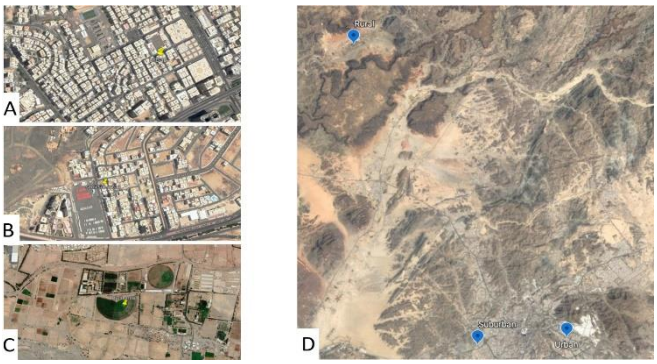

Fig. 4 A. Urban area; B. Suburban area; C. Rural area; D. Locations of the case study

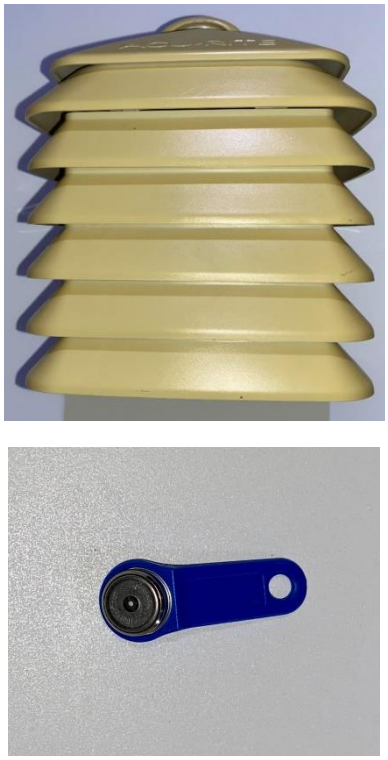

Fig. 5 Equipment used for on-site measurements

Table 2 The specification for the i-Button Data Loggers DS1923-F5

Model	Temperature Range	Accuracy	Resolution	Values/Readings	Logging Rate
DS1923 Hygrochron	-20°C to +85°C Includes 0 to 100% humidity logger	+/- 0.5°C: -10°C to +65°C (with software correction)	Programmable 0.5°C - 8bit / 0.0625°C - 11 bit	8192 - 8 bit or 4096 - 16 bit	1 sec to 273 hrs

Table 3 Information of all study locations

Area	Distance from urban area	Data measured	Tool of measurement
Urban	---	Temp. & RH	i-Button Data Logger (DS1923-F5)
Suburban	16.3 KM	Temp. & RH	i-Button Data Logger (DS1923-F5)
Rural	46 KM	Temp. & RH	Hada Al-sham metrological station.

The i-Button DS1923-F5 data loggers were tested to ensure their suitability for field assessment through a validation exercise conducted under a controlled environment in a specialized chamber at Universiti Kebangsaan Malaysia (UKM) laps, where the data loggers were used to record the temperature and relative humidity in the chamber. The equipment was placed on a table and set to measure simultaneously at 10-minute intervals in the chamber room, where the temperature was pre-set at 40 ℃ and 40% for relative humidity. A high accuracy range was recorded in the calibration of the i-Button DS1923-F5 with an average difference of 0.4℃ to 0.5℃ between chamber room conditions and the readings obtained from the equipment. This result corresponds with the accuracy stated in the manufacturer's specification. This calibration methodology was used in previous research [12, 62]. The result of the validation process is presented in Table 3. As for Hada Al-sham metrological station, it was significant to ensure that it had proper data values in the study. For this purpose, maintenance procedures, temperature, and relative humidity specifications were checked and found satisfactory. In addition, readings from the Hada Al-sham metrological station were also validated to ensure the accuracy of climatic data for the rural area. The process involves comparing temperature readings derived from the Hada Al-sham metrological station, with that recorded using the i-Button DS1923-F5 data loggers placed in the urban settlement during June 2019. The result reflects a high similarity in the trend line, which is logically acceptable. Visual representation of the result is presented in Figures 6-7.

Date - Time	Data logger 1	Data logger 2	Origin
18/03/2019 12:00	39.6	39.6	40 °C
18/03/2019 12:10	39.6	39.6	40 °C
18/03/2019 12:20	39.6	39.6	40 °C
18/03/2019 12:30	39.6	39.6	40 °C
18/03/2019 12:40	39.6	39.6	40 °C
18/03/2019 12:50	39.6	39.6	40 °C
18/03/2019 13:00	39.6	39.6	40 °C
18/03/2019 13:10	39.6	39.6	40 °C
18/03/2019 13:20	39.6	39.6	40 °C
18/03/2019 13:30	39.6	39.6	40 °C
18/03/2019 13:40	39.6	39.6	40 °C
18/03/2019 13:50	39.6	39.6	40 °C
18/03/2019 14:00	39.6	39.6	40 °C
18/03/2019 14:10	39.6	39.6	40 °C
18/03/2019 14:20	39.6	39.6	40 °C
18/03/2019 14:30	39.6	39.6	40 °C
18/03/2019 14:40	39.6	39.6	40 °C
18/03/2019 14:50	39.6	39.6	40 °C
18/03/2019 15:00	39.6	39.6	40 °C
18/03/2019 15:10	39.6	39.6	40 °C
18/03/2019 15:20	39.6	39.6	40 °C
18/03/2019 15:30	39.6	39.6	40 °C
18/03/2019 15:40	39.6	39.6	40 °C
18/03/2019 15:50	39.6	39.6	40 °C
18/03/2019 16:00	39.6	39.6	40 °C
Average of percentage difference	0.4	0.4	-

Fig. 6 Result of the validation test conducted on the i-Button Data Loggers DS1923-F5

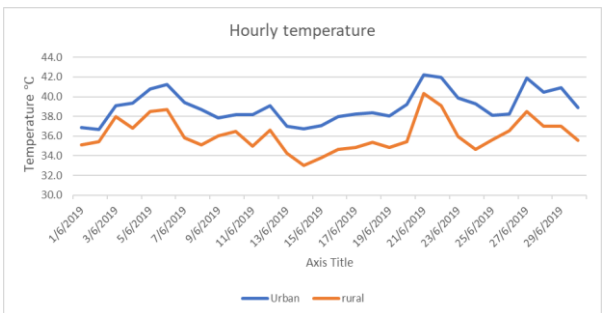

Fig. 7 Comparison of hourly temperature readings recorded in Hada Al-Sham metrological station and the i-Button data logger

3.3. Data Collection and Field Measurement

The air temperature or thermal environment in the urban context is usually measured using sensors positioned within the atmospheric layer of the urban area or urban boundary layer. The cumulative impact of the different components is measured from different sensors/stationed in the study area [18]. The general climatic condition of an area where the study is conducted is the first component, while the second component describes the geographic feature of the study area, e.g., mountain range, coastline, and elevation effect. The third component, referred to as the urban component, described the change in climate conditions resulting from urban growth [18]. The U.S. stated that the UHI phenomenon in an area that can be measured from the reading of surface temperature or ambient air temperature [63]. Surface temperatures can significantly influence air temperature, albeit indirectly, while close compaction of buildings in an area increases air temperature. To effectively characterize the impact of UHI in the city of Makkah, the study was conducted on three areas representing the urban, suburban, and rural environment. Climatic data for the study were collected in the year's hottest months: June, July, and August. In the urban and suburban areas, the i-Button Data Loggers DS1923-F5 was positioned at the height of 10 meters and implemented to be a free-standing object with a shield future. Data on ambient air temperature in the rural area was collected from Hada Al-sham metrological station. The weather station was selected after validation to ensure accuracy at the comparison phase. Air temperature information from the three-research locations was collected continually and simultaneously for June, July, and August with an interval of one hour. The site visit was conducted to inspect the iButton data loggers in the urban and suburban areas to check for technical problems or other issues.

4. Data Analysis of Field Measurements

The data analysis collected from field observation conducted in Makkah city is presented in this section. The UHII was studied from data collected on air temperature, including the mean daytime, nighttime, and daily average, using UHI as the dependent variable. UHI describes the difference in ambient air temperature between an urban environment and an adjoining rural area at a given time [24, 64]. For this study, UHI is defined as the difference in air temperature between a given area in Makkah and the rural measurement station at the same date and time. The methodology employed in this study was applicable in other parts of the world [65].

4.1. Daytime Average

The iButton data loggers were pre-set to record daytime air temperature reading from 6 AM until 6 PM in the summer months of June to August 2019. A significant difference was observed in Ta between the urban and rural locations. The value of variation in daytime air temperature between the rural area and the urban area was 3.6℃ in July, while 3.2℃ was the air temperature difference between the rural and suburban areas in the same time frame. The highest Ta was recorded in the urban and suburban environment with values of 44.5℃ and 51℃, respectively, observed on the 21st of June 2019. Meanwhile, the lowest Ta value in the rural area was 32.4 ℃ recorded on the 12th of August, whereas Ta of 33.5℃ and 32.6℃ was observed in the urban and suburban area on the same day.

Compared to their urban counterpart, comparably higher values of daytime Ta recorded in the suburban area could be ascribed to the difference in topography of the two areas. However, this effect did not result in higher nighttime Ta of the suburban area. The explanation for this will be provided in the subsequent section. Meanwhile, the Ta recorded in the rural area was significantly lesser than those recorded in the urban and suburban areas. The ambient daytime air temperature for all locations under study is presented in Figure 8.

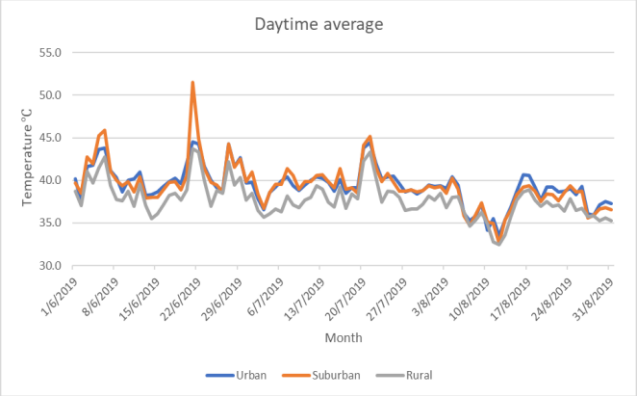

Fig. 8 Daytime Ta for all locations

4.2. Nighttime Average

At night, heat is usually emitted into the atmosphere from the surrounding built-up area, thereby creating a higher Ta, an occurrence reported being one of the major causes of the UHI condition [66, 67]. In several UHI investigation studies, researchers have proven that in urban areas, nocturnal Ta is mostly higher than diurnal Ta, which raises the significant effects of the UHI phenomena on the building performance as well as thermal comfort on the surrounding environment [28, 68]. In the present study, the readings on nighttime temperature were collected for 12 hours between 6 PM to 6AM with an interval of one hour. A great difference was observed in the Ta of the urban area compared to the rural area with a difference of 6.3℃, which was ascribed to the features of urban growth in the urban area. In contrast, nighttime Ta in the urban area was higher than in the suburban area, with a different value of 2.4℃. The highest Ta recorded in all the study locations was 40.4℃ in the urban area, while the lowest value was 28.5 ℃ observed in the rural area. In

comparing nighttime Ta among all locations, the maximum amount of Ta was observed in the urban environment. The nighttime Ta for all the locations is presented in Figure 9.

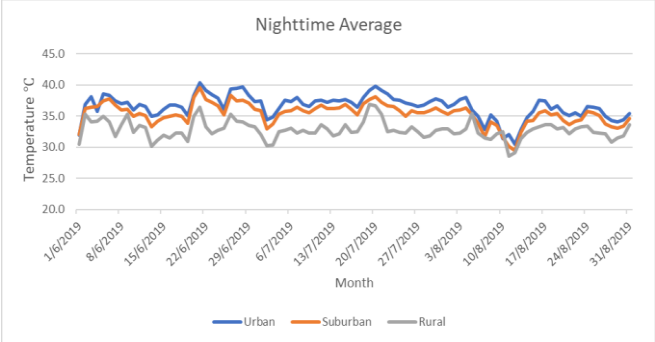

Fig. 9 Nighttime Ta for all locations

4.3. Daily Average

Daily average Ta was analyzed in this study to assess the impact of spatial variation on the microclimate of each area. To achieve this, the hourly ambient air temperature of each day was recorded, and the mean value of all readings was recorded as the daily Ta. In a comparison of the mean daily value of the Ta among the three representative areas, it was observed that the urban environment recorded the highest Ta value32.0 ℃ to 42.2 ℃ during the data collection period, while the highest difference in Ta value between the urban and suburban context was 4.6℃ recorded on the 24th of June 2019. The mean value of Ta among the studied location is illustrated in Figure 10.

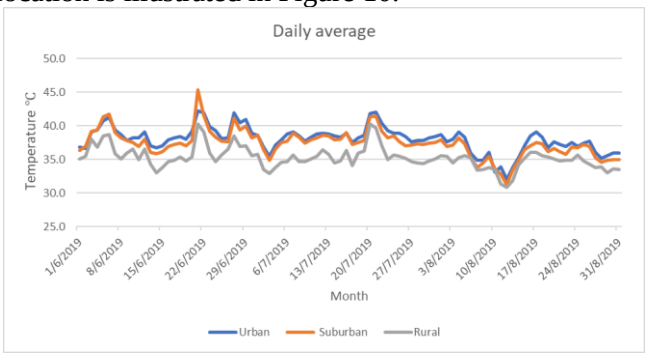

Fig. 10 Daily Ta average for all locations

Also, it was observed that the highest monthly Ta value was recorded in the urban area for the entire summer period, while June recorded the highest Ta value among all stations. The monthly ambient air temperature in all locations is illustrated in Figure 11.

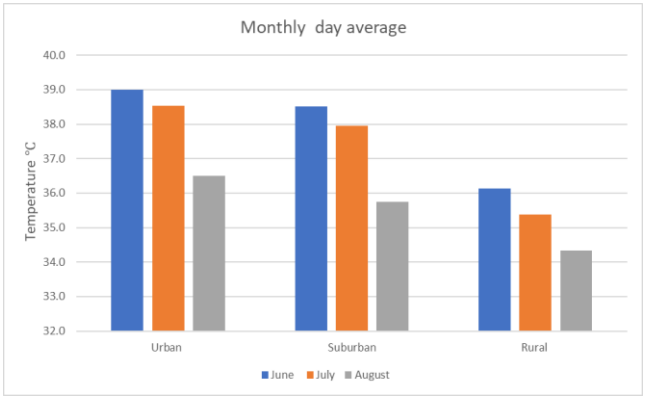

Fig. 11 Monthly day Ta for all locations

5. Discussion and Conclusion

The case of UHI phenomenon has been attributed to urban growth and development. A high level of growth in terms of infrastructure is usually experienced in the metropolitan owing to an increase in human population growth. Thus, urban centers usually have higher air temperatures than adjacent rural settlements within the same geographical boundaries [69, 70], and this difference in microclimate conditions is described as UHI [73]. Research has shown that UHI has a profound impact on the energy consumption of buildings [71, 72], in a review of past research on the effect of UHI on energy consumption in buildings, indicated that UHI can bring about up to a 19% rise in cooling energy demand [72].

Considering the microclimate in Makkah city, it was observed that there is high Ta variation among the study location. Nighttime temperature was highest in the urban area. The highest average nighttime Ta in the urban, suburban, and rural areas were 40.4℃, 39.6℃, and 36.5 ℃, respectively. The highest daytime difference in ambient air temperature was 3.6 ℃, observed between the urban and rural environments in June 2019. Although the suburban area recorded a higher daytime Ta than its urban counterpart, nighttime ambient air temperature was higher in the urban area with a difference value of 2.1℃.

Meanwhile, it was observed that nighttime temperature was higher in the urban area compared to the suburban area for the entire study duration. In June – August 2019, the urban environment recorded the highest daytime Ta among all locations under study. During the period under consideration, it was observed that daytime variation for Ta in the urban and suburban areas peaked at 4.6 ℃ and 3.7 ℃, respectively. Meanwhile, the urban area had the highest Ta values among the stations regarding monthly daytime Ta. From the data above analysis, it is clear that the city of Makkah experiences higher Ta in both daytime and nighttime in an urban area compared to the rural environment. This phenomenon is significant to be addressed as Makkah is experiencing more than a 40% increase in total energy consumption during the last decade [38]. Given that 1.18 GW is required for every ℃ one increase in the

temperature [32], continued Ta increase in the urban area will lead to a significant rise in energy consumption. To the best of our knowledge, there is a shortage of research focused on analyzing the urban heat island consequences and its mitigation in the city of Makkah.

The procedure of analyzing and investigating the actual characteristics of the microclimate within a given area is highly difficult to be comprehensively reported. Every second data representative cannot be accurately documented by any statistical approach [68]. In our study, part of the research limitation lies in the measurement of the morphological parameters. We used the air temperature variation between different locations in Makkah city as a description of the UHII, a methodology supported by other similar works [74, 75]. Another limitation is the positioning of measuring tools as suggested by WMO at 2 m from ground level was impossible to implement the data loggers at an approachable level since it could be lost.

Nevertheless, at the early stage of measurement, 2 m level was measured simultaneously with at 10 m level for ten days. A significant similarity was found between both measurement points with a calculated correlation coefficient, R^2, of 0.9907. Therefore, all data were corrected based on the differences of +0.1 °C.

The present study assessed the impact of UHI in the context of Makkah city by measuring urban heat island intensity at the urban, suburban, and rural areas during the summertime (June – August 2019). The study aim was fulfilled by examining the influence of air temperature outside the canyon as a parameter for measuring UHII. The information needed for this study was obtained through a campaign conducted to collect meteorological information from stations in each study location. Previous studies have identified the occurrence of UHI by the variation of Ta in the urban area of a specific city against its surrounding rural area [2, 76, 77, 78]. Analysis of the data collected confirmed that urban areas in Makkah city experience higher Ta than rural areas. This finding supports the fact of UHI existence at Makkah. The increase in air temperature observed in the study was related to the effect of urbanization. It is projected that the phenomenon will intensify to a greater extent in the future. The future work of this project will be extended by quantifying the influence of the UHI on building energy consumption via a dynamic simulation process. A typical dwelling will be selected and simulated in different micro-climate to study the impact of the UHI on the energy use of the selected dwelling.

References

[1] DUTTA I., and DAS A. Exploring the Spatio-temporal pattern of regional heat island (RHI) in an urban agglomeration of secondary cities in Eastern India, *Urban Clim.*, 2020, 34 (7): 100679, doi: 10.1016/j.uclim.2020.100679

[2] BERNARD J., MUSY M., CALMET I., BOCHER E., and KERAVEC P. Urban heat island temporal and spatial variations: Empirical modeling from geographical and meteorological data, *Build. Environ.*, Nov. 2017, 125: 423–438 doi: 10.1016/j.buildenv.2017.08.009

[3] MILLS G. Luke Howard and The Climate of London, 2018, no. August, doi: 10.1002/wea.195

[4] BAHI H., RHINANE H., BENSALMIA A., FEHRENBACH U., and SCHERER D. Effects of urbanization and seasonal cycle on the surface urban heat island patterns in the coastal growing cities: A case study of Casablanca, Morocco, *Remote Sens.*, 2016, 8 (10), doi: 10.3390/rs8100829

[5] BAHI H., RHINANE H., and BENSALMIA A. Contribution of MODIS satellite image to estimate the daily air temperature in the Casablanca City, Morocco, *Int. Arch. Photogramm. Remote Sens. Spat. Inf. Sci. - ISPRS Arch.*, 2016, 42 (2W1): 3–11, doi: 10.5194/isprs-archives-XLII-2-W1-3-2016

[6] YANG X., CHEN Y., PENG L. L. H., and WANG Q. Quantitative methods for identifying meteorological conditions conducive to the development of urban heat islands, *Build. Environ.*, 2020, 178 (4): 106953. doi: 10.1016/j.buildenv.2020.106953

[7] MOHAJERANI A., BAKARIC J., and JEFFREY-BAILEY T. The urban heat island effect, its causes, and mitigation, with reference to the thermal properties of asphalt concrete, *J. Environ. Manage.*, 2017, 197, (7): 522–538. doi: 10.1016/j.jenvman.2017.03.095

[8] STEWART I. D., and OKE T. R. Local climate zones for urban temperature studies, *Bull. Am. Meteorol. Soc.*, 2012, 93 (12): 1879–1900. doi: 10.1175/BAMS-D-11-00019.1

[9] LEE R. L., OLFE. Linearized calculations of urban heat island convection effects., *J. Atmos. Sci.*, 1971, 28:1374–13, [Online]. Available: http://library1.nida.ac.th/termpaper6/sd/2554/19755.pdf.

[10] SHEPHERD J. M., PIERCE H., and NEGRI A. J. Rainfall modification by major urban areas: Observations from spaceborne rain radar on the TRMM satellite, *J. Appl. Meteorol.*, 2002, 41 (7): 689–701. doi: 10.1175/1520-0450(2002)041<0689:RMBMUA>2.0.CO;2

[11] CHANGNON S. A., HUFF F. A., and SEMONIN R. G. METROMEX: an Investigation of Inadvertent Weather Modification, *Bull. Am. Meteorol. Soc.*, 1971, 52 (10): 958–968. doi: 10.1175/1520-0477(1971)052<0958:maioiw>2.0.co;2

[12] SKELHORN C. P., LEVERMORE G., and LINDLEY S. J. Impacts on cooling energy consumption due to the UHI and vegetation changes in Manchester, UK, *Energy Build.*, 2016, 122: 150–159, doi: 10.1016/j.enbuild.2016.01.035

[13] MUSCO F. et al. *UHI in the Metropolitan Cluster of Bologna- Modena: Mitigation and Adaptation Strategies*. Cham: Springer International Publishing, 2016.

[14] ZHOU Y., ZHUANG Z., YANG F., YU Y., and XIE X., Urban morphology on heat island and building energy consumption, *Procedia Eng.*, 2017, 205: 2401–2406. doi: 10.1016/j.proeng.2017.09.862

[15] WANG Y., BERARDI U., and AKBARI H. Comparing the effects of urban heat island mitigation strategies for Toronto, Canada, *Energy Build.*, 2016, 114: 2–19. doi: 10.1016/j.enbuild.2015.06.046

[16] BAKARMAN M. A. and CHANG J. D. The influence of height / width ratio on urban heat island in hot-arid climates, 2015, 118: 101–108. doi: 10.1016/j.proeng.2015.08.408

[17] KARL T. R., DIAZ H. F., and KUKLA G. Urbanization: Its Detection and Effect in the United States Climate Record, *J. Clim.*, 1988.
[18] BAHI H., MASTOURI H., and RADOINE H. Materials Today: Proceedings Review of methods for retrieving urban heat islands, *Mater. Today Proc.*, 2020, 27: 3004–3009. doi: 10.1016/j.matpr.2020.03.272
[19] EL BOUAZOULI A., BAIDDER L., PASQUIER P., and RHOUZLANE S. Remote sensing contribution to the identification of potential geothermal deposits: A case study of the Moroccan Sahara, *Mater. Today Proc.*, 2019, 13: 784–794. doi: 10.1016/j.matpr.2019.04.041
[20] SETO K. C., and CHRISTENSEN P. Remote sensing science to inform urban climate change mitigation strategies, *Urban Clim.*, 2013, 3: 1–6. doi: 10.1016/j.uclim.2013.03.001
[21] ABUHUSSAIN M. A., HOU D., CHOW C. H. I., and SHARPLES S. *PLEA 2018 HONG KONG Assessing the adaptability of the Saudi residential building ` s energy code for future climate change scenarios*, 2018.
[22] LIU L. et al. Analysis of local-scale urban heat island characteristics using an integrated method of mobile measurement and GIS-based spatial interpolation, *Build. Environ.*, 2017, 117: 191–207. doi: 10.1016/j.buildenv.2017.03.013
[23] STEWART I. D. A systematic review and scientific critique of methodology in modern urban heat island literature, *Int. J. Climatol.*, 2011, 31 (2): 200–217. doi: 10.1002/joc.2141
[24] DESPINI F. et al. Correlation between remote sensing data and ground based measurements for solar reflectance retrieving, *Energy Build.*, 2016, 114: 227–233. doi: 10.1016/j.enbuild.2015.06.018
[25] ZHOU D., ZHAO S., LIU S., ZHANG L., and ZHU C. Surface urban heat island in China's 32 major cities: Spatial patterns and drivers, *Remote Sens. Environ.*, 2014, 152: 51–61. doi: 10.1016/j.rse.2014.05.017
[26] KAMARIANAKIS Y., LI X., TURNER B. L., and BRAZEL A. J. On the effects of landscape configuration on summer diurnal temperatures in urban residential areas: application in Phoenix, AZ, *Front. Earth Sci.*, 2019, 13 (3): 445–463. doi: 10.1007/s11707-017-0678-4
[27] CUI Y., YAN D., HONG T., and MA J. Temporal and spatial characteristics of the urban heat island in Beijing and the impact on building design and energy performance, *Energy*, 2017, 130: 286–297. doi: 10.1016/j.energy.2017.04.053
[28] GUATTARI C., EVANGELISTI L., and BALARAS C. A. On the assessment of urban heat island phenomenon and its effects on building energy performance: A case study of Rome (Italy), *Energy Build.*, 2018, 158 (1): 605–615. doi: 10.1016/j.enbuild.2017.10.050
[29] SANTAMOURIS M., CARTALIS C., SYNNEFA A., and KOLOKOTSA D. On the impact of urban heat island and global warming on the power demand and electricity consumption of buildings - A review, *Energy Build.*, 2015, 98: 119–124. doi: 10.1016/j.enbuild.2014.09.052
[30] HOWARTH N., ODNOLETKOVA N., ALSHEHRI T., ALMADANI A., LANZA A., and PATZEK T. Staying Cool in A Warming Climate: Temperature, Electricity and Air Conditioning in Saudi Arabia, *Climate*, 2020, 8 (1): 4. doi: 10.3390/cli8010004
[31] KRARTI M., and HOWARTH N. Transitioning to high efficiency air conditioning in Saudi Arabia: A benefit cost analysis for residential buildings, *J. Build. Eng.*, 2020, 31 (4): 101457. doi: 10.1016/j.jobe.2020.101457
[32] KRARTI M., ALDUBYAN M., and WILLIAMS E. Residential building stock model for evaluating energy retrofit programs in Saudi Arabia, *Energy*, 2020, 195: 116980. doi: 10.1016/j.energy.2020.116980
[33] AL-AHMADI K., SEE L., HEPPENSTALL A., and HOGG J. Calibration of a fuzzy cellular automata model of urban dynamics in Saudi Arabia, *Ecol. Complex.*, 2009, 6 (2): 80–101. doi: 10.1016/j.ecocom.2008.09.004
[34] ALQURASHI A. F., and KUMAR L. Land Use and Land Cover Change Detection in the Saudi Arabian Desert Cities of Makkah and Al-Taif Using Satellite Data, *Adv. Remote Sens.*, 2014, 03 (03): 106–119. doi: 10.4236/ars.2014.33009
[35] ALQURASHI A. F., KUMAR L., and AL-GHAMDI K. A. Spatiotemporal modeling of urban growth predictions based on driving force factors in five Saudi Arabian Cities, *ISPRS Int. J. Geo-Information*, 2016, 5 (8). doi: 10.3390/ijgi5080139
[36] *G. Authority for Statistics. Electrical energy statistics 2018*, 2018. https://www.stats.gov.sa/en/1042 (accessed the 02nd of November, 2020).
[37] *G. Authority, for statistics, GASTAT: The total number of pilgrims in 1439H Hajj season reached (2.371.675) pilgrims*, 2021. https://www.stats.gov.sa/en/news/280 (accessed the 22nd of March, 2021).
[38] ALGAHTANI H. Strategic vision of planning the central area of Makkah City, *Islam. Herit. Archit. Art*, 2016, 1 (Iha): 107–120. doi: 10.2495/iha160101
[39] NATIONS ONLINE. *Satellite View and Map of the City of Mecca (Makkah al-Mukarramah)*, Saudi Arabia, 2021. https://www.nationsonline.org/oneworld/map/google_map_Mecca.htm (accessed the 01st of March, 2021).
[40] AL-GHAMDI K. Impacts of urban growth on flood hazards in Makkah City, Saudi Arabia, *... J. Water ...*, 2012, 4 (2): 23–34. doi: 10.5897/IJWREE11.128
[41] PEEL M. C., FINLAYSON B. L., and MCMAHON T. A. *Updated world map of the K ¨ oppen-Geiger climate classification*, 2007, 1633–1644.
[42] AL-AHMADI K., and AL-AHMADI S. Rainfall-Altitude Relationship in Saudi Arabia, *Adv. Meteorol.*, 2013, 3: 1–14, doi: 10.1155/2013/363029
[43] ABDOU A. E. A. Temperature Trend on Makkah, Saudi Arabia, *Atmos. Clim. Sci.*, 2014, 04 (03}: 457–481. doi: 10.4236/acs.2014.43044
[44] *World Weather & Climate Information. Climate in Mecca*, Saudi Arabia, 2021. https://weather-and-climate.com/average-monthly-Rainfall-Temperature-Sunshine,mecca-sa,Saudi-Arabia (accessed the 21st of March, 2021).
[45] CHERNIWCHAN, JEVAN. Economic growth, industrialization, and the environment, *Resource and Energy Economics*, 2012, Elsevier, 34(4): 442-467.
[46] LIU X., and BAE J. Urbanization and industrialization impact of CO2 emissions in China. *Journal of Cleaner Production,* 2018. DOI:10.1016/j.jclepro.2017.10.156
[47] MAHMOOD H., ALKHATEEB T. Role of education and economic growth on the CO2 emissions in Saudi Arabia. *Journal of Entrepreneurship and Sustainability Issues*, 2020, 8(2):195-209. DOI:10.9770/jesi.2020.8.2(12)
[48] BRITISH PETROLEUM. *Annual Report and Form 20-F 2020.*

https://www.bp.com/en/global/corporate/investors/results-and-reporting/annual-report.html
[49] ALSHEHRY A.S., AND BELLOUMI M. Energy consumption, carbon dioxide emissions and economic growth: The case of Saudi Arabia. *Renewable and Sustainable Energy Reviews*, 2015, 41: 237-247. DOI: 10.1016/j.rser.2014.08.004
[50] ALYOUSEF Y., and ABU-EBI M. Energy Efficiency Initiatives for Saudi Arabia on Supply and Demand Sides. *Energy Efficiency - A Bridge to Low Carbon Economy*, 2012, 279-308. https://doi.org/10.5772/38660
[51] YE X. et al. Evaluation and intercomparison of wildfire smoke forecasts from multiple modeling systems for the 2019 Williams Flats fire. Atmos. Chem. Phys., 2021, 21: 14427–14469.
https://doi.org/10.5194/acp-21-14427-2021
[52] GARSTANG T. P. M. The structure of heat islands, *Rev. Geophys.*, 1975, 13 (1): 139–165.
[53] OKE T. R. The energetic basis of the urban heat island, *Q. J. R. Meteorol. Soc.*, 1982, 108 (455): 1–24. doi: 10.1002/qj.49710845502
[54] DRAXLER R. R. Simulated and observed influence of the nocturnal urban heat island on the local wind field.," *Clim. Appl. Meteor.*, 25: 1125–2233, 1986, [Online]. Available: http://library1.nida.ac.th/termpaper6/sd/2554/19755.pdf
[55] LIN Y. L., and SMITH R. B. Transient dynamics of airflow near a local heat source., *J. Atmos. Sci.*, 1986, 43 (1): 40–49. doi: 10.1175/1520-0469(1986)043<0040:TDOANA>2.0.CO;2
[56] DEOSTHALI V. Impact of rapid urban growth on heat and moisture islands in Pune City, India, *Atmos. Environ.*, 2000, 34 (17): 2745–2754, doi: 10.1016/S1352-2310(99)00370-2
[57] CHANGNON, S. A., JR., HUFF, F. A., and SEMONIN, R. G. METROMEX: An investigation of inadvertent weather modification. *Bull. Amer. Meteor. Soc.*, 1971, 52: 958-968.
[58] GARTLAND L. Heat Islands: Understanding and mitigating heat in urban areas. London, Routledge, 2008. DOI:10.4324/9781849771559
[59] BAKARMAN MOHAMMED, AND CHANG J.D. The Influence of Height/width Ratio on Urban Heat Island in Hot-arid Climates. *Procedia Engineering*, 2015, 118: 101-108. DOI:10.1016/j.proeng.2015.08.408
[60] KOLOKOTRONI M., ZHANG Y., and WATKINS R. The London Heat Island and building cooling design, 2007, 81: 102–110. doi: 10.1016/j.solener.2006.06.005
[61] SUNDBORG, Å. Local climatological studies of the temperature conditions in an urban area, *Tellus*, 1950, 2: 221-31.
[62] CHEUNG HENRY KEI WANG. Electrical Probes for Study of Two-Phase Flows, *Univ. Manchester*, 2011, 68–70.
[63] *United States Environmental Protection Agency, Measuring Heat Islands*, 2019. https://www.epa.gov/heatislands/measuring-heat-islands (accessed the 11th of November,2020)
[64] PARKINSON C. J. B., LAYCOCK P. J., and LINDLEY S. The urban heat island in Manchester 1996-2011, *Build. Serv. Eng. Res. Technol.*, 36 (3): 343–356, 2015, doi: 10.1177/0143624414549388
[65] KOLOKOTRONI M. and GIRIDHARAN R. Urban heat island intensity in London: An investigation of the impact of physical characteristics on changes in outdoor air temperature during summer, *Sol. Energy*, 2008, 82 (11): 986–998. doi: 10.1016/j.solener.2008.05.004
[66] KARDINAL JUSUF S., WONG N. H., HAGEN E., ANGGORO R., and HONG Y. The influence of land use on the urban heat island in Singapore, *Habitat Int.*, 2007, 31 (2): 232–242. doi: 10.1016/j.habitatint.2007.02.006
[67] LIU Y., LI Q., YANG L., MU K., ZHANG M., and LIU J. Urban heat island effects of various urban morphologies under regional climate conditions, *Sci. of the Total Environ.*, 2020, 743. doi: 10.1016/j.scitotenv.2020.140589.
[68] YANG X. et al. Assessing the thermal behavior of different local climate zones in the Nanjing metropolis, China, *Build. Environ.*, 2018, 137 (30): 171–184. doi: 10.1016/j.buildenv.2018.04.009
[69] SANTAMOURIS M. et al. On the impact of urban climate on the energy consuption of building. *Solar Energy*, 2001, 70 (3): 201-216. DOI:10.1016/S0038-092X(00)00095-5
[70] HOWARTH C., BRYANT P., FANKHAUSER S., and CORNER A. Building a Social Mandate for Climate Action: Lessons from COVID-19. Environmental and Resource Economics 76(3), 2020. DOI:10.1007/s10640-020-00446-9
[71] PALME M., INOSTROZA L., VILLACRESES G., LOBATO-CORDERO A., and CARRASCO C. From urban climate to energy consumption. Enhancing building performance simulation by including the urban heat island effect, *Energy Build.*, 2017, 145: 107–120. doi: 10.1016/j.enbuild.2017.03.069
[72] LI X., ZHOU Y., YU S., JIA G., LI H., and LI W. Urban heat island impacts on building energy consumption: A review of approaches and findings, *Energy*, 2019, 174: 407–419. doi: 10.1016/j.energy.2019.02.183
[73] HUANG Q., HUANG J., YANG X., FANG C., AND LIANG Y. Quantifying the seasonal contribution of coupling urban land use types on Urban Heat Island using Land Contribution Index: A case study in Wuhan, China, *Sustain. Cities Soc.*, 2018, 44 (5): 666–675. doi: 10.1016/j.scs.2018.10.016.
[74] PARKER J. The Leeds urban heat island and its implications for energy use and thermal comfort, *Energy Build.*, 2020, 7: 110636. doi: 10.1016/j.enbuild.2020.110636
[75] KOLOKOTRONI M., AND WATKINS R. The effect of the London urban heat island on building summer cooling demand and night ventilation strategies. *Solar Energy*, 2006, 80(4): 383-392. DOI:10.1016/j.solener.2005.03.010
[76] FANCHIOTTI A., CARNIELLO E., and ZINZI M. Impact of Cool Materials on Urban Heat Islands and on Buildings Comfort and Energy Consumption," *Wref*, 2012, 1–8. [Online]. Available: http://ases.conference-services.net/resources/252/2859/pdf/SOLAR2012_0176_full paper.pdf
[77] RICHARDS D. R., FUNG T. K., BELCHER R. N., and EDWARDS P. J. Differential air temperature cooling performance of urban vegetation types in the tropics, *Urban For. Urban Green.*, 2020, 50 (3). doi: 10.1016/j.ufug.2020.126651
[78] BOKAIE M., ZARKESH M. K, ARASTEH P. D., and A. HOSSEINI. Assessment of Urban Heat Island based on the relationship between land surface temperature and Land Use/ Land Cover in Tehran, *Sustain. Cities Soc.*, 2016, 23: 94–104. doi: 10.1016/j.scs.2016.03.009

参考文:

[1] DUTTA I., 和 DAS A. 探索印度東部二級城市城市群區域熱島 (RHI) 的時空格局，城市气候., 2020, 34 (7): 100679, doi: 10.1016/j.uclim.2020.100679.
[2] BERNARD J., MUSY M., CALMET I., BOCHER E., 和 KERAVEC P. 城市熱島時空變化：基於地理和氣象數據的經驗建模，建造。環境，十一月. 2017, 125: 423–438 doi: 10.1016/j.buildenv.2017.08.009.
[3] MILLS G. 盧克霍華德和倫敦的氣候，2018, 不。 八月, 土井: 10.1002/wea.195.
[4] BAHI H., RHINANE H., BENSALMIA A., FEHRENBACH U., 和 SCHERER D. 城市化和季節循環對沿海城市地表熱島模式的影響：以摩洛哥卡薩布蘭卡為例，遙感，2016, 8 (10), 土井: 10.3390/rs8100829.
[5] BAHI H., RHINANE H., 和 BENSALMIA A. MODIS 衛星圖像對估計摩洛哥卡薩布蘭卡市每日氣溫的貢獻。拱。攝影。遙感。吐。信息科學。- ISPRS 拱門，2016, 42 (2宽1): 3–11, 土井: 10.5194/isprs-archives-XLII-2-W1-3-2016.
[6] YANG X., CHEN Y., PENG L. L. H., 和 WANG Q. 識別有利於城市熱島發展的氣象條件的定量方法，構建。環境，2020, 178 (4): 106953. 土井: 10.1016/j.buildenv.2020.106953.
[7] MOHAJERANI A., BAKARIC J., 和JEFFREY-BAILEY T. 城市熱島效應、其成因和緩解，參考瀝青混凝土的熱性能，J. 环境。管理。，2017, 197, (7): 522–538. 土井: 10.1016/j.jenvman.2017.03.095.
[8] STEWART I. D., 和 OKE T. R. 用於城市溫度研究的當地氣候區，公牛。是。 氣象。 社會，2012, 93 (12): 1879–1900. doi: 10.1175/BAMS-D-11-00019.1.
[9] LEE R. L., OLFE. 城市熱島對流效應的線性計算。J. 大气。科學，1971, 28:1374–13, [在線的]。可用的: http://library1.nida.ac.th/termpaper6/sd/2554/19755.pdf.
[10] SHEPHERD J. M., PIERCE H., 和 NEGRI A. J. 主要城市地區的降雨修正：TRMM 衛星上星載降雨雷達的觀測結果，J. 应用程序。氣象，2002, 41 (7): 689–701. 土井: 10.1175/1520-0450(2002)041<0689:RMBMUA>2.0.CO;2.
[11] CHANGNON S. A., HUFF F. A., 和 SEMONIN R. G. 美特美：無意中改變天氣的調查，公牛。是。氣象。社會，1971, 52 (10): 958–968. 土井: 10.1175/1520-0477(1971)052<0958:maioiw>2.0.co;2.
[12] SKELHORN C. P., LEVERMORE G., 和 LINDLEY S. J. 英國曼徹斯特的 UHI 和植被變化對冷卻能源消耗的影響，能源建设。2016, 122: 150–159, 土井: 10.1016/j.enbuild.2016.01.035.
[13] MUSCO F. 等。博洛尼亞-摩德納都市集群中的 UHI：緩解和適應策略。占: 施普林格国际出版, 2016.
[14] ZHOU Y., ZHUANG Z., YANG F., YU Y., 和 XIE X.. 熱島城市形態與建築能耗，继续工程，2017, 205: 2401–2406. 土井: 10.1016/j.proeng.2017.09.862.
[15] WANG Y., BERARDI U., 和 AKBARI H. 比較加拿大多倫多的城市熱島緩解策略的效果，能源建設，2016, 114: 2–19. 土井: 10.1016/j.enbuild.2015.06.046.
[16] BAKARMAN M. A. 和 CHANG J. D. 高寬比對炎熱乾旱氣候下城市熱島的影響，2015, 118: 101–108. 土井: 10.1016/j.proeng.2015.08.408.
[17] KARL T. R., DIAZ H. F., 和 KUKLA G. 城市化：它在美國氣候記錄中的檢測和影響，J. 气候.， 1988.
[18] BAHI H., MASTOURI H., 和 RADOINE H. 今日材料：檢索城市熱島方法的論文集回顧，母校。今天程序，2020, 27: 3004–3009. 土井: 10.1016/j.matpr.2020.03.272.
[19] EL BOUAZOULI A., BAIDDER L., PASQUIER P., 和 RHOUZLANE S. 遙感對潛在地熱礦床識別的貢獻：摩洛哥撒哈拉沙漠的案例研究，馬特。 今天程序，2019, 13: 784–794. 土井: 10.1016/j.matpr.2019.04.041.
[20] SETO K. C., 和 CHRISTENSEN P. 遙感科學為城市氣候變化減緩戰略提供信息，城市氣候，2013, 3: 1–6. 土井: 10.1016/j.uclim.2013.03.001.
[21] ABUHUSSAIN M. A., HOU D., CHOW C. H. I., 和 SHARPLES S. 恳求2018 香港評估沙特住宅建築能源規範對未來氣候變化情景的適應性，2018.
[22] LIU L. 等。使用移動測量和基於地理信息系统的空間插值的綜合方法分析局部尺度的城市熱島特徵，建造。環境，2017, 117: 191–207. 土井: 10.1016/j.buildenv.2017.03.013.
[23] STEWART I. D. 現代城市熱島文獻中方法論的系統回顧和科學批判，整数。J. 气候醇., 2011, 31 (2): 200–217. 土井: 10.1002/joc.2141.
[24] DESPINI F. 等。遙感數據與地面測量太陽反射率反演的相關性，能源建設，2016, 114: 227–233. 土井: 10.1016/j.enbuild.2015.06.018.
[25] ZHOU D., ZHAO S., LIU S., ZHANG L., 和 ZHU C. 中國 32 個主要城市的地表城市熱島：空間格局和驅動因素，遙感。 環境，2014, 152: 51–61. 土井: 10.1016/j.rse.2014.05.017.
[26] KAMARIANAKIS Y., LI X., TURNER B. L., 和 BRAZEL A. J. 景觀配置對城市居民區夏季晝夜溫度的影響：在鳳凰城、亞利桑那州、前線的應用。地球科學，2019, 13 (3): 445–463. 土井: 10.1007/s11707-017-0678-4.
[27] CUI Y., YAN D., HONG T., 和 MA J. 北京城市熱島時空特徵及其對建築設計和能源性能的影響，能源，2017, 130: 286–297. 土井: 10.1016/j.energy.2017.04.053.
[28] GUATTARI C., EVANGELISTI L., 和 BALARAS C. A. 關於城市熱島現象的評估及其對建築能源性能的影響：以羅馬（意大利）為例，能源建築，2018, 158 (1): 605–615. 土井: 10.1016/j.enbuild.2017.10.050.
[29] SANTAMOURIS M., CARTALIS C., SYNNEFA A., 和 KOLOKOTSA D. 關於城市熱島和全球變暖對建築物電力需求和電力消耗的影響——綜述，能源建設，2015, 98: 119–124. 土井: 10.1016/j.enbuild.2014.09.052.
[30] HOWARTH N., ODNOLETKOVA N., ALSHEHRI T., ALMADANI A., LANZA A., 和 PATZEK T. 在變暖的氣候中保持涼爽：沙特阿拉伯的溫度、電力和空調、氣候、2020, 8 (1): 4. 土井: 10.3390/cli8010004.
[31] KRARTI M., 和 HOWARTH N. 在沙特阿拉伯過渡到高效空調：住宅建築的收益成本分析，J. 建造。英文，2020, 31 (4): 101457. 土井: 10.1016/j.jobe.2020.101457.
[32] KRARTI M., ALDUBYAN M., 和 WILLIAMS E. 用於評估沙特阿拉伯能源改造計劃的住宅建築存量模型，能源，2020, 195: 116980. 土井: 10.1016/j.energy.2020.116980.
[33] AL-AHMADI K., SEE L., HEPPENSTALL A., 和 HOGG J. 沙特阿拉伯城市動力學模糊元胞自動機模型的校準，生态。 複雜的。，2009, 6 (2): 80–101. 土井: 10.1016/j.ecocom.2008.09.004.

[34] ALQURASHI A. F., 和 KUMAR L. 使用衛星數據對沙特阿拉伯沙漠城市麥加和塔伊夫的土地利用和土地覆蓋變化進行檢測，高级。遙感，2014, 03 (03): 106–119. 土井: 10.4236/ars.2014.33009.
[35] ALQURASHI A. F., KUMAR L., 和 AL-GHAMDI K. A. 基於沙特阿拉伯五個城市驅動力因素的城市增長預測時空模型，ISPRS 国际。J. 地理信息，2016, 5 (8). 土井: 10.3390/ijgi5080139.
[36] G. 統計局。2018 年電能統計，2018. https://www.stats.gov.sa/en/1042 (2020 年 11 月 2 日访问).
[37] G. 權威，用於統計，加斯达：總計1439H 朝覲季節的朝聖者人數達到 (2.371.675) 朝圣者.，2021. https://www.stats.gov.sa/en/news/280 (2021 年 3 月 22 日访问).
[38] ALGAHTANI H. 規劃伊斯蘭教麥加市中心區的戰略願景。繼承。建築。藝術，2016, 1 (伊哈): 107–120. 土井: 10.2495/iha160101.
[39] 国家在线. 沙特阿拉伯麥加市 (麦加穆卡拉玛) 的衛星視圖和地圖，2021. https://www.nationsonline.org/oneworld/map/google_map_Mecca.htm (accessed the 01st of March, 2021).
[40] K. AL-GHAMDI. 沙特阿拉伯麥加市城市發展對洪水災害的影響，J. 水，2012, 4 (2): 23–34. 土井: 10.5897/IJWREE11.128.
[41] PEEL M. C., FINLAYSON B. L., 和 MCMAHON T. A. 更新了科彭-盖格氣候分類的世界地圖，2007, 1633–1644.
[42] AL-AHMADI K., 和 AL-AHMADI S. 沙特阿拉伯的降雨-海拔關係，高级. 氣象，2013, 3: 1–14, 土井: 10.1155/2013/363029.
[43] ABDOU A. E. A. 麥加、沙特阿拉伯、大气的**溫**度趨勢。氣候。科學，2014, 04 (03}: 457–481. 土井: 10.4236/acs.2014.43044.
[44] 世界天氣和氣候信息。沙特阿拉伯麥加的氣候2021. https://weather-and-climate.com/average-monthly-Rainfall-Temperature-Sunshine,mecca-sa,Saudi-Arabia (2021 年 3 月 21 日访问).
[45] CHERNIWCHAN, JEVAN. 經濟增長、工業化和環境、資源和能源經濟學 2012, 爱思唯尔, 34(4): 442-467.
[46] LIU X., **和** BAE J. 中國城市化和工業化對二氧化碳排放的影響。清潔生產雜誌，2018. DOI:10.1016/j.jclepro.2017.10.156
[47] MAHMOOD H., ALKHATEEB T. 教育和經濟增長對沙特阿拉伯二氧化碳排放量的作用。創業與可持續性問題雜誌, 2020, 8(2):195-209. DOI:10.9770/jesi.2020.8.2(12)
[48] 英国石油公司。2020 年年度报告和 20-F 表格。https://www.bp.com/en/global/corporate/investors/results-and-reporting/annual-report.html
[49] ALSHEHRY A.S., 和 BELLOUMI M. 能源消耗、二氧化碳排放和經濟增長：以沙特阿拉伯為例。可再生和可持續能源評論，2015, 41: 237-247. DOI: 10.1016/j.rser.2014.08.004
[50] ALYOUSEF Y., 和 ABU-EBI M. 沙特阿拉伯供需雙方的能源效率倡議。能源效率 - 低碳經濟的橋樑, 2012, 279-308. https://doi.org/10.5772/38660
[51] YE X. **等。**對 2019 年威廉姆斯平底鞋火災的多個建模系統的野火煙霧預測進行評估和比對。大氣。化學 物理, 2021, 21: 14427–14469. https://doi.org/10.5194/acp-21-14427-2021
[52] GARSTANG T. P. M. 熱島的結構，地球物理學博, 1975, 13 (1): 139–165.
[53] OKE T. R. 城市熱島的能量基礎，问. J. 电阻. 陨石。社會，1982, 108 (455): 1–24. doi: 10.1002/qj.49710845502.
[54] DRAXLER R. R. 模擬和觀察到的影響當地風場上的夜間城市熱島。” 气候. 應用程序 流星25: 1125–2233, 1986, [在線的]。可用的：http://library1.nida.ac.th/termpaper6/sd/2554/19755.pdf.
[55] LIN Y. L., 和 SMITH R. B. 局部熱源附近氣流的瞬態動力學。J. 大气。科學，1986, 43 (1): 40–49. 土井: 10.1175/1520-0469(1986)043<0040:TDOANA>2.0.CO;2.
[56] DEOSTHALI V. 城市快速增長對印度浦那市熱濕島的影響，大气。環境，2000, 34 (17): 2745–2754, 土井: 10.1016/S1352-2310(99)00370-2.
[57] CHANGNON, S. A., JR., HUFF, F. A., 和 SEMONIN, R. G. 美特美：對無意影響天氣的調查。公牛。阿米爾。流星。社會，1971, 52: 958-968.
[58] GARTLAND L. 熱島：了解和減輕城市地區的熱量。倫敦，勞特利奇, 2008. DOI:10.4324/9781849771559
[59] BAKARMAN MOHAMMED, 和 CHANG J.D. 高/寬比對炎熱乾旱氣候下城市熱島的影響。继续工程，2015, 118: 101-108. DOI:10.1016/j.proeng.2015.08.408
[60] KOLOKOTRONI M., ZHANG Y., 和 WATKINS R. 倫敦熱島和建築冷卻設計，2007, 81: 102–110. 土井: 10.1016/j.solener.2006.06.005.
[61] SUNDBORG, Å. 告诉我们市區**溫**度條件的局部氣候學研究, 1950, 2: 221-31.
[62] CHEUNG HENRY KEI WANG. 用於研究兩相流的電探針，大學。曼徹斯特，2011, 68–70. 美國環境保護署，測量熱島，2019. https://www.epa.gov/heatislands/measuring-heat-islands (2020 年 11 月 11 日訪問).
[63] 美國環境保護署，測量熱島, 2019.
[64] PARKINSON C. J. B., LAYCOCK P. J., 和 LINDLEY S. 1996-2011 年曼徹斯特的城市熱島，建造。服務。英。水庫技術，36 (3): 343–356, 2015, 土井: 10.1177/0143624414549388.
[65] KOLOKOTRONI M. 和 GIRIDHARAN R. 倫敦城市熱島強度：夏季物理特**徵**對室外氣**溫**變化影響的調查，溶胶. 活力，2008, 82 (11): 986–998. 土井: 10.1016/j.solener.2008.05.004.
[66] KARDINAL JUSUF S., WONG N. H., HAGEN E., ANGGORO R., 和 HONG Y. 土地利用對新加坡城市熱島的影響，人居國際，2007, 31 (2): 232–242. 土井: 10.1016/j.habitatint.2007.02.006.
[67] LIU Y., LI Q., YANG L., MU K., ZHANG M., 和 LIU J. 區域氣候條件下各種城市形態的城市熱島效應，科學。整個環境的.，2020, 743. 土井: 10.1016/j.scitotenv.2020.140589.
[68] YANG X. 等。評估中國南京大都市不同地方氣候帶的熱行為，構建。環境, 2018, 137 (30): 171–184. 土井: 10.1016/j.buildenv.2018.04.009
[69] SANTAMOURIS M. 等。城市氣候對建築能耗的影響[J]. 太陽能, 2001, 70 (3): 201-216. DOI:10.1016/S0038-092X(00)00095-5

[70] HOWARTH C., BRYANT P., FANKHAUSER S., 和 CORNER A. 建立氣候行動的社會使命：來自新冠肺炎的教訓。環境與資源經濟學 76(3), 2020. DOI:10.1007/s10640-020-00446-9
[71] PALME M., INOSTROZA L., VILLACRESES G., LOBATO-CORDERO A., 和 CARRASCO C. 從城市氣候到能源消耗。通過包括城市熱島效應、能源建築，增強建築性能模擬，2017, 145: 107–120. 土井：10.1016/j.enbuild.2017.03.069.
[72] LI X., ZHOU Y., YU S., JIA G., LI H., 和 LI W. 城市熱島對建築能耗的影響：方法和發現的回顧，能源，2019, 174: 407–419. 土井: 10.1016/j.energy.2019.02.183.
[73] HUANG Q., HUANG J., YANG X., FANG C., 和 LIANG Y. 使用土地貢獻指數量化城市熱島耦合城市土地利用類型的季節性貢獻：以中國武漢為例，维持。城市社會2018, 44 (5): 666–675. 土井: 10.1016/j.scs.2018.10.016.
[74] PARKER J. 利茲城市熱島及其對能源使用和熱舒適性的影響，能源建設。2020, 7: 110636. 土井：10.1016/j.enbuild.2020.110636.
[75] KOLOKOTRONI M., 和 WATKINS R. 倫敦城市熱島對建築夏季降溫需求和夜間通風策略的影響。太陽能，2006, 80(4): 383-392. DOI:10.1016/j.solener.2005.03.010
[76] FANCHIOTTI A., CARNIELLO E., 和 ZINZI M. 冷材料對城市熱島和建築舒適度和能源消耗的影響，”参考文献，2012，1-8。[在線的]。可用的：http://ases.conference-services.net/resources/252/2859/pdf/SOLAR2012_0176_fullpaper.pdf.
[77] RICHARDS D. R., FUNG T. K., BELCHER R. N., 和 EDWARDS P. J. 熱帶城市植被類型的差溫降溫性能，城市为。城市綠化，2020, 50 (3). 土井：10.1016/j.ufug.2020.126651.
[78] BOKAIE M., ZARKESH M. K, ARASTEH P. D., 和 A. HOSSEINI. 基於地表溫度與德黑蘭土地利用/土地覆蓋之間關係的城市熱島評估，维持。城市社會，2016, 23: 94–104. doi: 10.1016/j.scs.2016.03.009.